Ion velocity distributions at the tokamak edge

R. A. Pitts

Citation: Phys. Fluids B 3, 2871 (1991); doi: 10.1063/1.859919
View online: http://dx.doi.org/10.1063/1.859919
View Table of Contents: http://pop.aip.org/resource/1/PFBPEI/v3/i10
Published by the American Institute of Physics.

Ion velocity distributions at the tokamak edge

R. A. Pitts
AEA Fusion, Culham Laboratory, UKAEA/Euratom Fusion Association, Abingdon, Oxfordshire OX14 3DB, United Kingdom

(Received 29 March 1991; accepted 31 May 1991)

This paper compares the form of $f(v_\parallel)$ arising from the warm-ion, kinetic models of Emmert *et al.* [Phys. Fluids **23**, 803 (1980)] and Bissel and Johnson [Phys. Fluids **30**, 779 (1987)] with experimentally measured distributions from the DITE tokamak obtained with a retarding field analyzer (RFA). The results show that the commonly adopted assumption of a distribution accelerated through the sheath potential and approximating to a Maxwellian in the high-energy tail is reasonable. In this respect, Emmert's distribution is more appropriate. In addition, the common practice of neglecting the presheath effect on the distribution is generally justified in analyzing the RFA characteristic, but may incur large error under some circumstances. While the comparison also illustrates how differing assumptions regarding the source function can have a reasonably strong influence on the ion velocity distribution at walls and limiters, the integrated distributions required for comparison with RFA data are sufficiently similar that distinguishing between the models experimentally is not generally possible. The problems of resolving these differences experimentally are discussed and suggestions are proposed for further experiments.

I. INTRODUCTION

The problem of modeling plasma flow along magnetic field lines to the tokamak limiter or divertor plate has been the subject of much theoretical work.[1-13] Because the flow is unimpeded by the field, the situation is inherently one-dimensional and may be approached from a kinetic[1-10] or fluid[10-13] point of view, neglecting the magnetic field. Each method leads to predictions for the spatial variation of flow speed, potential, density, etc., in the presheath, or scrape-off layer (SOL) plasma.

While both the kinetic and fluid approaches often lead to similar estimates for quantities of important practical interest,[10] unlike the fluid treatments kinetic models can also be used to compute the form of the ion velocity distribution at any point in the flow. In particular, they provide the form of the distribution parallel to **B**, $f(v_\parallel)$, at the plasma/sheath interface and the solid surface. Knowledge of the latter is important for accurate characterization of the ion–surface interaction. For example, it has been pointed out that the details of $f(v_\parallel)$ at high velocities can have a marked influence on the feasibility of certain candidate fusion reactor first wall materials.[14] The ability to predict theoretically the form of $f(v_\parallel)$ is also significant in the sense that it can be directly measured and hence used to compare experiment and theory. Such measurements are possible using the technique of retarding field energy analysis in which a probe inserted into the tokamak edge extracts ions and energy analyzes them using electric fields.[15-17]

Since the SOL plasma is usually characterized by ion temperatures close to or exceeding the electron temperature, it is most appropriate to use warm ion kinetic models in comparing with experiment. Of these, the collisionless treatments presented by Emmert *et al.*[2] and Bissel and Johnson[3] contain convenient analytic forms for $f(v_\parallel)$. They are also of particular interest since each uses a different, but similar, assumption for the form of the source ion velocity distribution $f_s(v_\parallel)$. While this does not greatly affect important measurable quantities such as density and potential at the wall,[10] it has rather more influence on the shape of $f(v_\parallel)$.

This paper attempts to examine the validity of these warm ion source terms as prescriptions for the source distribution in the tokamak edge by comparing the predicted velocity distributions at the absorbing surface with those measured in the edge plasma of the DITE tokamak[18] using a retarding field analyzer (RFA). In Sec. II the kinetic models to be used are briefly summarized, with emphasis on the predicted velocity distributions. In Sec.III the RFA is described and experimental integral distributions are presented which, in Sec. IV, are compared with those presented in differential form below. Conclusions are offered in Sec. V.

II. KINETIC MODELING

In most treatments of plasma flow to surfaces, the plasma is assumed to be contained in a one-dimensional planar geometry bounded by "walls" or perfectly absorbing surfaces at $x = \pm L$ that are electrically floating. Kinetic treatments of ion flow to a surface formulate and solve a plasma equation describing the variation of plasma potential, $\phi_p(x)$, in a direction normal to the plane of the walls ($\phi_p = 0$ at $x = 0$ is normally assumed). This potential exists to accelerate ions through the plasma to the solid surface such that, at the sheath edge, the ion velocity distribution satisfies the generalized Bohm criterion.[19]

In deriving the plasma equation (valid up to the plasma/sheath interface), a form for the electron and ion density must be specified. The electrons are assumed to obey a Boltzmann distribution:

$$n_e(x) = n_e(0)\exp[e\phi_p(x)/kT_e], \tag{1}$$

where $n_e(0)$ is the electron density at $x = 0$, while in colli-

 0899-8221/91/102871-06$02.00

sionless treatments (collisionless with respect to ion–ion collisions), the ion density is obtained from a solution to the kinetic equation for the conservation of particles

$$\frac{d}{dx}\left[v_{\parallel} f(v_{\parallel},x)dv_{\parallel}\right] = S_p(v_{\parallel},x)dv_{\parallel}, \tag{2}$$

where S_p is the ion source function. Although the methods of solution and assumed boundary conditions vary from one model to the next, it is essentially the form adopted for S_p which determines the major differences between the predictions of each model. Studies in which some forms of collisions are included are more complex since the full Boltzmann kinetic equation must be solved with some assumption for the form of the collision term.[8,9] The degree to which a collisionless approximation is valid in the tokamak presheath can be debated. In DITE, the relatively low edge density and short connection length mean that such an assumption is almost always justified. In machines with longer connection length such as JET,[20] collisionless conditions may only be attained for very low densities when the edge temperature is highest.

Tonks and Langmuir[1] gave the first collisionless analysis but assumed either that the ions were cold ($T_s = 0; T_s$ the ion source temperature) or that their temperature was finite but small ($T_s \ll T_e$). Of more relevance to the edge plasma of fusion devices are the warm ion sources in which T_s can assume any value.

Emmert *et al.*[2] considered a source of the form

$$S_p(x,v_{\parallel}) = H(x)f_s(v_{\parallel}) = H(x)\frac{m_i v_{\parallel}}{2kT_s}\exp\left(-\frac{m_i v_{\parallel}^2}{2kT_s}\right), \tag{3}$$

where $H(x)$ is the spatial variation of the source strength. Singly charged ions are assumed and the plasma is taken to have zero net drift velocity. In Emmert's study $H(x)$ was taken as constant along the presheath region, although an assumption regarding the source profile is not required to evaluate the form of the distribution functions shown below. Equation (3) is in the form of a flux and describes a source which, in the absence of electric fields in the plasma, would give rise to a Maxwellian ion velocity distribution. Physically this is so because ions are lost to the walls at a rate proportional to their velocity and so the source must produce the faster particles faster if the number density is to be kept up to Maxwellian. This is provided for by the velocity weighting factor in Eq. (3).

Bissel and Johnson[3] assumed a slightly different source

$$S_p(x,v_{\parallel}) = H(x)f_s(v_{\parallel}) = H(x)\frac{m_i}{2kT_s}\exp\left(-\frac{m_i v_{\parallel}^2}{2kT_s}\right), \tag{4}$$

which represents, for example, the source that would arise from the velocity independent ionization of a Maxwellian distribution of neutrals at temperature T_s ($H(x)$ is assumed proportional to the electron density in the presheath). Unlike the Emmert source, the use of Eq. (4) in the plasma equation does not lead to a Maxwellian ion velocity distribution. The differences are evident in Fig. 1 which shows the source distributions, $f_s(v_{\parallel})$ given by Eqs. (3) and (4). The absence of a zero velocity component gives Emmert's distribution a distinctive double-humped feature.

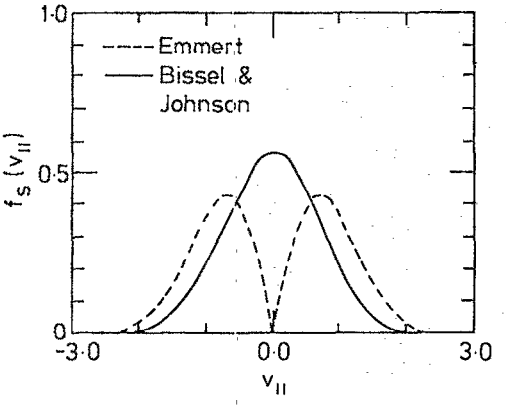

FIG. 1. Illustrating the form of $f_s(v_{\parallel})$ assumed by Emmert *et al.*[2] and Bissel and Johnson[3] (from Bissel *et al.*[8])

Once an equation describing $\phi_p(x)$ has been established, the ion distribution function may be calculated explicitly at any point for a given value of the ratio T_s/T_e and ion charge state, Z_i. Figure 2 illustrates the normalized forms of $f(v_{\parallel})$ at $x = \phi_p = 0$ arising from each source for singly charged ions for $T_s/T_e = 1$. The curves show very clearly how the Bissel and Johnson source leads to a very different distribution with fewer fast ions and more slow ions in comparison to the Emmert distribution.

At the sheath edge, Emmert's distribution, f_{se}^{E}, may be written in simplified form in terms of the normalized parallel velocity, $u^2 = m_i v_{\parallel}^2/2kT_s$ and potential $\psi = -e\phi_p/kT_e$

$$f_{se}^{E}(u)du \propto \frac{1}{Z_i T_s^{1/2}}\exp\left(\frac{Z_i\psi_0}{\tau}\right)A\,du, \tag{5}$$

where $\psi_0 = \psi_{se} - u^2, \tau = T_s/T_e$, and with

$$A = \begin{cases} 1 + F(\psi_{se}) - 2F(\psi_0), & 0 < u < u_{se} \\ 1 + F(\psi_{se}), & u > u_{se} \end{cases}$$

$$u_{se} = (Z_i\psi_{se}/\tau)^{1/2},$$

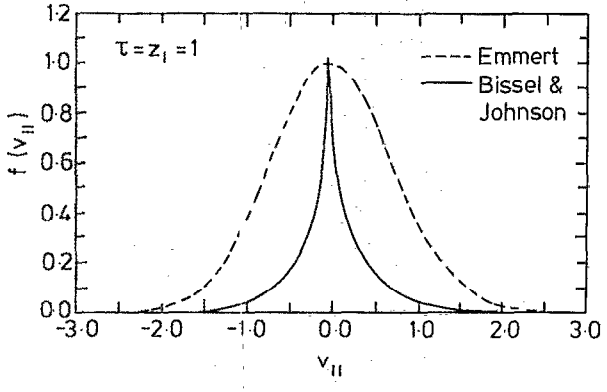

FIG. 2. Normalized ion velocity distributions, $f(v_{\parallel})$, at the stagnation point ($x = \phi_p = 0$) arising from the source distributions in Fig. 1.

where F is a complex function of Z_i, τ and ψ_{se}, u_{se} is the velocity gained by an ion released at $x = 0$ and accelerated to the plasma/sheath boundary and ψ_{se} is the normalized sheath edge potential. An extra velocity interval, $u < 0$, would have to be considered for values of $\psi > \psi_{se}$, but this is not required for the sheath edge distribution since there can be no backward going ions at this point.

The Bissel and Johnson distribution at the sheath edge, f_{se}^{BJ}, is defined in terms of the normalized velocity $w^2 = m_i v_{\parallel}^2 / 2kT_e$ and takes the form

$$f_{se}^{BJ}(w)dw \propto \int_0^{\psi_{se}} d\psi \times f(\psi) \frac{e^{\psi} \exp[-1/\tau(w^2 + \psi_{se} - \psi)]}{(w^2 + \psi_{se} - \psi)^{1/2}} dw, \tag{6}$$

if $w^2 > \psi_{se}$ and where $f(\psi) = ds/d\psi$ is the inverse of the presheath electric field (s is the normalized distance, x/L). When $w^2 > \psi_{se}$, the lower limit of the integral becomes $w^2 + \psi_{se}$. Note that the variable τ in Eqs. (5) and (6) is defined differently from that in the papers by Emmert and Bissel and Johnson where, in both cases, $\tau = T_e/T_s$ is used.

Although the plasma equation is not valid in the sheath, the distribution at the wall, $f_w(v_{\parallel})$, may be computed from that at the sheath edge by applying conservation of energy

$$\tfrac{1}{2} m_i v_w^2 = \tfrac{1}{2} m_i v_{se}^2 + Z_i k T_e (\psi_w - \psi_{se}) \tag{7}$$

under the assumption of a sheath sufficiently thin that the source may be neglected there. This criterion is easily satisfied in the tokamak SOL where the Debye length, λ_D, is typically $\sim 25 \rightarrow 50\,\mu$m[15] compared with a presheath dimension of several meters. Both f_{se}^{E}, f_{se}^{BJ} and the accelerated distributions, f_w^{E}, f_w^{BJ}, at the absorbing surface for the case $\tau = Z_i = 1$ are shown in Fig. 3. Each distribution has been normalized to unity and the same sheath acceleration has been used in both cases for comparative purposes (the actual sheath potential fall, $V_s = \phi_{se} - \phi_w$, predicted by each model is slightly different).

As the distributions are accelerated through the presheath and into the sheath they become bunched in velocity space but still retain the essential features evident at $x = 0$ (Fig. 2). Differences between the models in the shape of the distributions during the velocity interval corresponding to ion acceleration through the presheath alone are also evident. This region is identified as that encompassing all velocities up to the peak in the distributions; its shape is determined by the presheath potential and source distributions. For the Bissel and Johnson case, the presence of a large proportion of slower ions means that the presheath potential must be larger than that in Emmert's model in order to satisfy the Bohm criterion. The magnitude and shape of this presheath interval has important consequences for the interpretation of retarding field analyzer characteristics to be described below.

III. EXPERIMENT

The retarding field analyzer (RFA), shown schematically in Fig. 4, provides a simple means of measuring the ion velocity distribution in the tokamak edge.[15-17] Ions enter the device through a small, negatively biased or electrically floating slit and experience a retarding electric field due to a positive voltage applied to a grid electrode (a separate, negatively biased grid is used to remove unwanted electrons). The ion repeller voltage may be ramped from 0 to some large positive value such that the *integral* of the ion velocity distribution is obtained. By aligning the analyzer normal to the tokamak magnetic field, the parallel component of the ion velocity may be observed. The delicate internal components are commonly housed within a protective graphite case of dimension comparable to the main limiters. Provided the slit width is sufficiently small that the sheath is able to bridge the gap and hence shield it from the plasma (i.e., $\sim \lambda_D$), the ion velocity distributions measured by the probe will be reasonably representative of those experienced at the limiters.[15]

Example current–voltage characteristics obtained in the DITE edge are shown in Fig. 5. The data are presented by

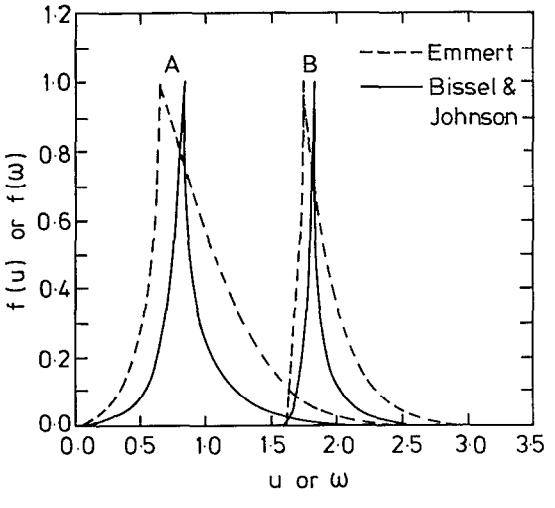

FIG. 3. Normalized Emmert and Bissel and Johnson ion velocity distributions at the sheath edge (A) and at the wall (B) as a function of normalized velocity for $\tau = Z_i = 1$.

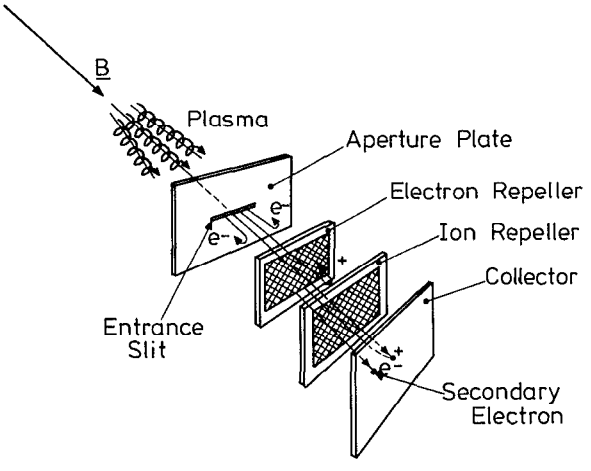

FIG. 4. Principle of the retarding field analyzer.

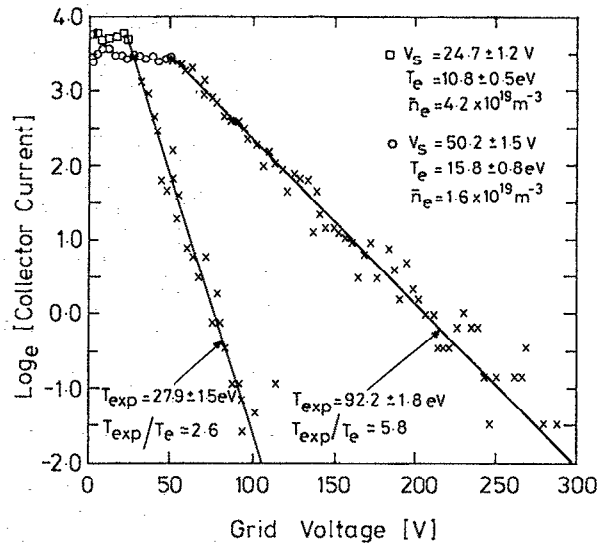

FIG. 5. Experimental RFA characteristics from the DITE tokamak obtained at two different times in the same, rising density helium discharge. Plasma conditions as in the figure and the text. Electron temperatures quoted are those measured at the RFA position during a separate identical discharge.

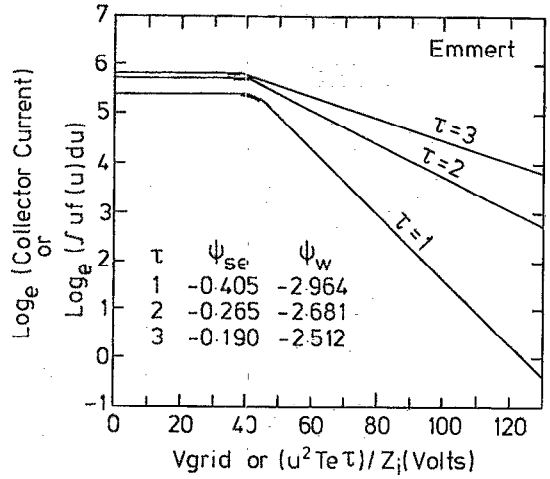

FIG. 6. Theoretical RFA characteristics arising from integration of Emmert's velocity distribution at the wall (Fig. 3) for three values of the ratio T_s/T_e with $Z_i = 1$ and $T_e = 15$ eV. Here ψ_{se} and ψ_w are the normalized potentials at the sheath edge and wall, respectively.

convention on a log-linear scale and two characteristics are shown, corresponding to two different times in the same Ohmic, rising density helium discharge with plasma current, $I_p = 115$ kA, and toroidal magnetic field, $B_T = 1.8$ T. The experimental characteristics show a very clear saturated region at low ion repeller voltages which is identified as due to acceleration in the sheath and presheath electric fields. At higher grid voltages the current decreases roughly exponentially. The full lines in Fig. 5 are the result of a nonlinear least squares fit to the data assuming the ion velocity distribution to be a one-dimensional Maxwellian beyond a voltage corresponding to the maximum energy gained in falling through the sheath and presheath potentials. That is,

$$I_c = I_0 \exp(Z_i V_g / T_{\exp}), \tag{8}$$

where I_c is the collector current and V_g is the retarding grid voltage. In Eq. (8) and Fig. 5, the variable $T_{\exp}$ has been used to denote the "experimental" ion temperature derived from the characteristic. The fitting has been performed for a fixed charge state of $Z_i = 2$.

As the plasma density increases, the edge electron and fitted ion temperatures decrease[15] but the ion temperature decrease is more dramatic, leading to a reasonably large change in the ratio of $T_{\exp}/T_e$. It is also notable that as the electron temperature decreases, the measured sheath potential also falls. This behavior has been shown elsewhere to be in good agreement with theoretical expectation provided that secondary electron emission is taken into account.[15,21]

IV. COMPARISON WITH THEORY

Direct comparison of the theoretical distributions of Fig. 3 with the characteristics of Fig. 5 requires differentiation of the experimental data or integration of the predicted forms. Unfortunately, the experimental noise level is sufficient that differentiation can introduce artificial features which complicate any comparison. In this case, a better approach is to reconstruct, by integration of $f_w(v_\parallel)$, the expected RFA characteristics for each model. This has been performed for the Emmert and Bissel and Johnson distributions by numerical integration of the analytic expressions in Eqs. (5) and (6).

The results are shown in Figs. 6 and 7 where it should be noted that the ordinate is actually the integral $\int uf(u)$ or $\int wf(w)$ since the RFA collector current really represents an ion flux. In both cases $T_e = 15$ eV has been arbitrarily assumed and the current at $V_g = 0$ chosen to be similar for

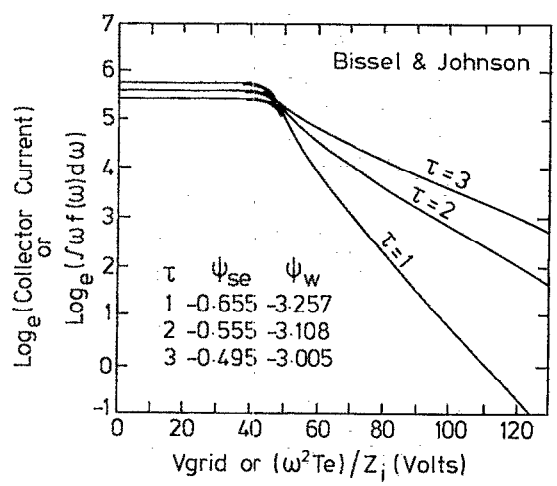

FIG. 7. Theoretical RFA characteristics arising from integration of Bissel and Johnson's velocity distribution at the wall (Fig. 3) for three values of the ratio T_s/T_e with $Z_i = 1$ and $T_e = 15$ eV. Here ψ_{se} and ψ_w are the normalized potentials at the sheath edge and wall, respectively.

comparative purposes. In all cases the region of the characteristic due to ion acceleration in the presheath has been highlighted. The curves for $\tau = 1,2,3$ and $Z_i = 1$ only are shown and the magnitude of the sheath energy gain has been calculated from each model. Since secondary electron emission is not considered in these kinetic models, the calculated values of V_s will not generally coincide with experimental observation.[15]

With regard to analysis of experimental characteristics, the integral distributions illustrate the difficulty of extracting information regarding the presheath potential fall. With the exception of the Bissel and Johnson curve at $\tau = 1$, there is very little curvature or "rounding off" of the characteristic before the current begins to decrease rapidly. As shown by the experimental curves in Fig. 5, the normal level of scatter in the data is sufficient to mask these small effects. Indeed, no strong evidence for the presheath has been found in any of the DITE experimental RFA characteristics. Of course, at higher values of τ, Figs. 6 and 7 indicate that any effect would be difficult to detect, particularly if Emmert's model were more appropriate. In the latter, as T_s increases, the presheath potential fall rapidly decreases since less voltage is required to accelerate the hotter ions to near sonic speeds at the sheath edge. Of course, the same is also true of the Bissel and Johnson model, but, because their source contains ions with zero velocity, the presheath potential will always have to be larger to satisfy the same criterion, whatever the source temperature.

Although the presheath interval appears in Figs. 6 and 7 to make a relatively small contribution to the total energy shift, this will not necessarily be the case in the presence of strong secondary electron emission. When this occurs, the sheath potential can fall dramatically[15] while the presheath voltage drop remains virtually unchanged. This poses a problem in deriving V_s from the experimental characteristics since it is not possible to distinguish the presheath contribution. In practice the presheath is ignored during the fitting process.

In the context of experimental data interpretation, the behavior of the theoretical characteristics in the high-energy tail is also very interesting. As implied by Eq. (5), Emmert's distribution decreases exponentially for all τ, while the Bissel and Johnson curves fall with a steeper gradient just in the small interval of grid voltage following the presheath zone. This is again just a consequence of the larger proportion of lower velocity ions and hence of the choice of source function.

At higher grid voltages the Bissel and Johnson characteristics decrease exponentially but the "effective" value of the ion temperature that would be deduced from a fit to these characteristics is lower than that actually assumed in generating them. This latter point emphasizes the problem of assigning an ion temperature in fitting the experimental characteristic. Of course, it is not strictly correct to refer to a temperature at all unless the particle velocity distribution is Maxwellian. In this sense, the variable T_s appearing in the source terms of Eqs. (3) and (4) should be regarded more as a model parameter characterizing the source than as an actual temperature. For example, even at the symmetry point where $\phi_p = 0$, a fully kinetic treatment gives $T_{i_\parallel} \simeq 0.4 T_s$ for the Bissel and Johnson source.[11] In Emmert's model, the distribution at $x = 0$ is actually a Maxwellian as shown in Fig. 2, and, in fact, if the Emmert source were physically the correct prescription, then the tail of the RFA characteristics *would* be a direct measure of T_s. Such differences arise simply as a consequence of the source functions—Emmert's source actually transports twice as much energy per particle in the parallel direction than the Bissel and Johnson source (the perpendicular energy per particle, $kT_{i\perp}$, is the same in both models).

Unfortunately, although differences in the theoretical integral distributions are evident, it is not possible to draw firm conclusions regarding the validity of either model from the experimental data in Fig. 5. While the data appear to decrease exponentially at higher grid voltages, there is, at least in the characteristic for which $T_{\exp}/T_e = 5.8$, some slight curvature away from a pure straight line decrease. Such effects can actually be attributed to a high-impurity concentration in the analyzed flux,[15,20] but would not produce the kind of dependence in the presheath region predicted by Bissel and Johnson (Fig. 7). This, of course, is the most important velocity interval in terms of distinguishing experimentally between the two models. Despite the relatively high noise level, strong evidence for the kind of behavior predicted for the Bissel and Johnson source has not been detected in any of the experimental RFA characteristics obtained in DITE.

Ultimately, any test of these kinetic models with the RFA will be limited by the problem of using an integral technique. Because the high level of fluctuations characteristic of the tokamak edge does not permit straightforward differentiation, one is restricted to comparing experiment and theory in the manner attempted in this paper. Although Figs. 5–7 imply that the experimental distribution may be reasonably described by either model, for the purposes of modeling ion interaction with surfaces in the tokamak, it is clear that assuming a one-dimensional, accelerated Maxwellian distribution will not invoke large error in any calculation. Furthermore, since the manner in which particles appear in the edge plasma is in any case anomalous and not understood, it is not clear that either of the source functions considered in these models is appropriate.

While the results presented here are not conclusive, it should be possible to obtain improved measurements. In the case of the RFA, future experiments should concentrate on the presheath region of the characteristic by restricting the grid voltage scan and increasing the sampling rate. Noise levels could be minimized by averaging a large number of sweeps during steady-state plasma conditions or even by modulating the scan voltage and using a lock-in amplifier detection system. The competing effects of impurities should be reduced by operating in edge plasmas with low Z_{eff}. In addition, since the presheath interval is a more important factor at the lowest values of τ, measurements should be made at the highest plasma densities, where this ratio is lowest.[15,21] In gettered tokamaks, at least, this density regime also coincides with the lowest impurity concentration.[22]

Clearly, a more desirable approach would be to measure

the energy distribution directly without the need for differentiation. $\mathbf{E}\times\mathbf{B}$ probes[23,24] do provide continuous monitoring of the parallel distribution, but the resolution is coarse compared to the retarding field analyzer. Alternative electrostatic focusing techniques, such as parallel plate analyzers, are difficult to use in a magnetic field—miniaturized devices are required in order to avoid complications due to finite Larmor radius and particle drifts. Spectroscopic methods are also possible; in particular, optical tagging[25] using laser-induced fluorescence measures the velocity distribution function without perturbing the plasma and so can monitor $f(v_\parallel)$ at points other than the solid surface. However, the technique is extremely complex in comparison with the simple RFA and cannot be used to measure the fuel ion distribution function in hydrogenic discharges.

As a final comment, it is important to note that no attempt has been made to compare experiment with alternative warm ion kinetic models available at this time. Chung and Hutchinson[6] follow Hutchinson's earlier fluid theory[13] in incorporating particle exchange between presheath and main plasma into a kinetic treatment which also allows for a net drift velocity, u_d, of the ion distribution function. They choose a Maxwellian velocity distribution in the plasma bounding the presheath but give no explicit analytic form for the ion distribution function. Their distributions at the wall appear qualitatively similar to those in Fig. 2 for $u_d = 0$, with greater differences becoming manifest at nonzero drift velocities. Scheuer and Emmert[8] have used Emmert's source function in a kinetic treatment including ion–ion and ion–neutral collisions. They compute the distribution function numerically but the shape of $f_w(v_\parallel)$ differs little from the collisionless case shown in Fig. 3. Schwager and Birdsall[7] choose a Maxwellian plasma source but their source is localized in a plane at $x = 0$. In this respect, it is not clear that their work is applicable to the tokamak edge.

V. CONCLUSIONS

While there have been many attempts to formulate a kinetic model of ion flow in the tokamak scrape-off layer, little or no effort has been made to investigate the validity of each study. One way in which this may be accomplished is to compare the ion velocity distributions expected at an absorbing surface with those measured in the tokamak edge. This is possible by integrating the theoretical distributions so that they may be directly compared with retarding field analyzer current–voltage characteristics.

Measurements from the DITE tokamak have been compared with the predictions of two recent warm-ion, collisionless kinetic models due to Emmert *et al.*[2] and Bissel and Johnson[3] in which different forms for the source ion velocity distribution are assumed. While these assumptions have a reasonably strong influence on the accelerated distributions at the solid surface, the integral forms, required for comparison with experimental RFA data, are not sufficiently different that absolute conclusions can be drawn regarding the applicability of each source to the real tokamak edge. In general, though, the departures from a pure Maxwellian high-energy tail predicted by the Bissel and Johnson model are not observed in the experimental data.

Nevertheless, the simple approximation of a one-dimensional Maxwellian distribution shifted in velocity space by acceleration through the sheath is a reasonable representation of the experimental data. Using this assumption in modeling ion interaction with surfaces at the tokamak edge is unlikely to introduce large errors compared with similar calculations employing the more complex distributions predicted theoretically. In terms of analyzing the experimental characteristics, the comparison also shows that, in general, the RFA cannot distinguish between the effects on the distribution of the sheath and presheath potential falls. However, the common practice of ignoring the presheath in the analysis may not be justified when secondary electron emission is high or the temperature is low.

Although ambient noise levels in the tokamak edge are generally large enough to obscure the small effects sought in comparing the models with experiment using the RFA, it should be possible to improve resolution and decrease the importance of signal fluctuations under certain conditions. In particular, experiments should be pursued in edge plasmas with low impurity concentration and in high-density discharges where the edge temperatures are lowest.

ACKNOWLEDGMENTS

The author is indebted to Dr. G. M. McCracken for encouragement and guidance, to Dr. P. C. Stangeby for useful discussions on the kinetic modeling, and to Dr. R. C. Bissel for permission to use parts of his software in formulating the integral distributions of Fig. 7.

[1] L. Tonks and I. Langmuir, Phys. Rev. **34**, 876 (1929).
[2] G. A. Emmert, R. M. Wieland, A. T. Mense, and J. N. Davidson, Phys. Fluids **23**, 803 (1980).
[3] R. C. Bissel and P. C. Johnson, Phys. Fluids **30**, 779 (1987).
[4] D. J. Koch and W. N. G. Hitchon, Phys. Fluids B **1**, 2239 (1989).
[5] J. T. Scheuer and G. A. Emmert, Phys. Fluids **31**, 3645 (1988).
[6] K. S. Chung and I. H. Hutchinson, Phys. Rev. A **38**, 4721 (1988).
[7] L. A. Schwager and C. K. Birdsall, Phys. Fluids B **2**, 1057 (1990).
[8] J. T. Scheuer and G. A. Emmert, Phys. Fluids **31**, 1748 (1988).
[9] K. U. Riemann, Phys. Fluids **24**, 2163 (1981).
[10] R. C. Bissel, P. C. Johnson, and P. C. Stangeby, Phys. Fluids B **1**, 1133 (1989).
[11] J. T. Scheuer and G. A. Emmert, Phys. Fluids B **2**, 445 (1990).
[12] P. C. Stangeby, Phys. Fluids **27**, 2699 (1984).
[13] I. H. Hutchinson, Phys. Fluids **30**, 3777 (1987).
[14] R. Behrisch, in Proceedings of the IAEA Workshop on Plasma Surface Interaction Data for Nuclear Fusion, to be published in Nucl. Fusion.
[15] R. A. Pitts, Ph.D thesis, University of London, 1991.
[16] G. F. Matthews, J. Phys. D **17**, 2243 (1984).
[17] A. S. Wan, T. F. Yang, B. Lipschultz, and B. LaBombard, Rev. Sci. Instrum. **57**, 1542 (1986).
[18] J. W. M. Paul and the DITE team, in *Plasma Physics and Controlled Nuclear Fusion Research, 1976* (IAEA, Vienna, 1977), Vol. II, p. 269.
[19] E. R. Harrison and W. B. Thompson, Proc. Phys. Soc. London **74**, 145 (1959).
[20] R. J. Bickerton and the JET team, Plasma Phys. Controlled Fusion **10A**, 1219 (1987).
[21] G. F. Matthews, R. A. Pitts, G. M. McCracken, and P. C. Stangeby, submitted to Nucl. Fusion.
[22] J. Winter, J. Nucl. Mater **176&177**, 14 (1990).
[23] G. F. Matthews, J. Phys. D **17**, 2243 (1984).
[24] P. Staib, J. Nucl. Mater. **111&112**, 109 (1982).
[25] F. Skiff, F. Anderegg, and M. Q. Tran, Phys. Rev. Lett. **58**, 1430 (1987).